

Superconductivity of topological insulator Bi₂Se₃ at high pressures

P. P. Kong, J. L. Zhang, S. J. Zhang, J. Zhu, Q. Q. Liu, R. C. Yu, Z. Fang, C. Q. Jin*

Beijing National Laboratory for Condensed Matter Physics, and Institute of Physics, Chinese Academy of Sciences, Beijing, 100190, China

W. G. Yang

High Pressure Synergetic Consortium (HPSynC) and High Pressure Collaborative Access Team (HPCAT), Geophysical Laboratory, Carnegie Institution of Washington, Argonne, Illinois 60439, United States

X. H. Yu, J. L. Zhu, Y. S. Zhao

Los Alamos Neutron Science Center (LANSCE), Los Alamos National Laboratory, Los Alamos, New Mexico 87545, United States

Abstract

The pressure-induced superconductivity and structural evolution for Bi₂Se₃ single crystal have been studied. The emergence of superconductivity with onset transition temperature (T_c) about 4.4K is observed around 12GPa. T_c increases rapidly to the highest 8.5K at 16GPa, decreases to 6.5K at 21GPa, then keep almost constant. It is found that T_c versus pressure is closely related to the carrier density which increases by more than two orders of magnitude from 2GPa to 23GPa. High pressure synchrotron radiation measurements reveal structure transitions occur around 12GPa, 20GPa, and above 29GPa, respectively. A phase diagram of superconductivity versus pressure is obtained.

Topological insulator (TI) with a bulk band gap but gapless edge state protected by time-reversal symmetry is a current frontier in condensed matter physics, attracting worldwide research interests.¹⁻⁸ There are many useful properties expected for topological compounds, ranging from new physics of Majorana Fermion,⁹ prospective applications of topological computer¹⁰, to exotic topological superconductors.¹¹ Recently a group three dimensional TIs of Bi₂Te₃, Bi₂Se₃, etc., are predicated, consequently observed by experiments such as angle-resolved photoemission spectroscopy (ARPES).^{4, 7, 11-13}

Similar to TI, topological superconductor has a full pairing gap in the bulk and gapless edge state consisting of elusive Majorana fermions.¹⁴ When topological insulator combines with magnetic or superconducting materials, Majorana state can be realized at its interface. Several application^{12, 15, 16} of interface between a topological insulator and a superconductor also have been proposed. The superconductivity of Bi₂Se₃ was observed via copper intercalating into the van der Waals gaps between the quintuple layers,¹⁷ while Bi₂Te₃ becomes superconductive at pressure.¹⁸ Pressure is much effective in generating or tuning superconductivity by modifying electronic structure through directly changing interatomic distance without introducing defects or impurities comparing with chemical doping. Here we report studies on the effects of pressure on Bi₂Se₃, We found that Bi₂Se₃ becomes superconducting at its high pressure phase.

Single crystal Bi₂Se₃ was grown by Bridgeman method. The details are described in Ref. 18. High purity elements Bi (99.999%) and Se (99.999%) were mixed in a molar ratio of 2:3, ground and pressed into pellets, then loaded into a quartz Bridgeman ampoule, which was

evacuated and sealed. The ampoule was placed in a furnace and heated at 800°C for 2 days, after that it was slowly cooled down at rate 3°C per hour to 550°C, kept for 3 days, then slowly cooled down to room temperature. The product was cleaved easily along the basal plane. The powder of Bi₂Se₃ ground from single crystal was identified by X-ray powder diffraction.

We measured the resistance of Bi₂Se₃ single crystal at high pressure by four-probe methods in a diamond anvil cell (DAC) made of CuBe alloy as described in Ref. 18, 19. To avoid the electrode leads contacting with the metallic gasket, cubic boron nitride (cBN) fine powders were covered on the gasket made of T301 stainless steel. The electrodes are slim Au wires with 18μm in diameter. The gasket, preloaded from the thickness of 250μm to 60μm, was drilled a hole of 250 micrometer diameter wherein cBN insulating layer was pressed to place the transmission medium hexagonal BN (hBN). The culet of the diamond anvil is about 500 micrometer. The dimension of Bi₂Se₃ single crystals for resistance experiments was about 70μm*70μm*10μm with soft hBN fine powders around as pressure transmitting medium. The pressure was determined by ruby fluorescence method.^{20,21} The diamond anvil cell was put inside a MagLab system to perform the experiments. To make sure the equilibrium of temperature, the temperature decreased slowly and was automatically controlled by the MagLab system. A thermometer nearby the diamond in the diamond anvil cell monitored the sample temperature accurately. The Hall coefficient at high pressure was measured by using Van der Pauw method.

The X-ray diffractions with synchrotron radiation at high pressure and low temperature using a symmetric Mao Bell diamond anvil cell were done at the HPCAT of Advanced Photon Source (APS) of Argonne National Lab (ANL) with a wavelength 0.398Å. The two-dimensional

image plate patterns are converted to one-dimensional 2θ versus intensity data using Fit2D software package.

Bi_2Se_3 , whose structure is the same as that of Bi_2Te_3 , has a nearly idealized single Dirac cone and the largest band-gap (approximately 0.3eV) among aforementioned 3D TIs.^{6,7} Bi_2Se_3 is a direct gap semiconductor,¹³ but strong spin-orbit coupling inverts the bulk bands at Γ point.⁶ There are some previous reports about effects of pressure on Bi_2Se_3 .^{22,23} Here we measured the transport property of Bi_2Se_3 single crystal in diamond anvil cell (DAC) via increasing the pressure for several times using different specimens. The behaviors of Bi_2Se_3 under high pressure are highly repetitive. The carrier density for the Bi_2Se_3 single crystals is around $2 \times 10^{18} \text{cm}^{-3}$ at ambient pressure when the temperature is 30K. Since the vacancy of selenium causes Fermi surface above the bottom of conduction-band, Bi_2Se_3 is of n type carriers.

Figure 1 presents the temperature dependence of resistance at different pressures over an extensive range, measured in the a-b plane while monotonically increasing pressure. Figure 1(a) shows the temperature dependence of resistance at ambient pressure phase with small pressure interval. When pressure is below 3.1GPa, Bi_2Se_3 displays weak metallic behavior. It becomes more metallic above 5.1GPa, which is probably related to the pressure-induced electronic topological transition (ETT) in Bi_2Se_3 near 5GPa as reported.²³ The behavior change of the sample at ambient phase is similar to the report in the Ref. 22. To confirm the resistance behavior is repeatable, we measured specimens from different batches as shown figure (b) and (c), respectively. Figure (b) illustrates the resistance versus temperature with big pressure interval. The general trend of the resistance is metallic, semiconducting and metallic, which is the same to

the results of figure 1 (a). More interesting, we observed clear superconducting transitions among several experiments. It is found that resistance drop firstly occur around 12GPa with the onset temperature (T_c) at about 4.4K. The T_c is defined using the same method described in Ref. 18, which is based on the differential of resistance over temperature. The selenium vacancy concentration can make the resistance and carrier density at ambient pressure vary by several orders of magnitude.²⁴ Different initial carrier density could be the origin of the somewhat different temperature dependences of the resistance from Ref22. We assume that a relative higher carrier density such in the level above 10^{18}cm^{-3} would be crucial to generate superconductivity in Be_2Se_3 . The evolution of resistance as a function of temperature at low temperature from 12.5GPa to 31.9GPa is shown in figure 1(c). The onset temperature with a clear resistive drop fleetly increases to the highest temperature of 8.5K, then decreases, and then keeps almost a constant by further increasing the pressure.

To assure whether the resistive drop is indeed a superconducting transition, we measured the transition temperature at variant external magnetic fields. Figure 2 shows the measured resistance in low temperature range at 23GPa with applied magnetic field H perpendicular to the a-b plane of single crystal (a). Increasing magnetic field, the onset temperature shifts toward lower temperature and finally zero resistance is lost at higher magnetic field, which is strong evidence that the transition is superconductivity in nature. The change of magnetic field H with superconducting transition temperature (T_c) is shown in the figure 2 (b). Using the

Werthdamer-Helfand-Hohenberg formula²⁴, $H_{c2} = -0.691 \times \left[\frac{dH}{dT} \right]_{T=T_c} \times T_c$, the upper

critical field $H_{c2}(0)$ is extrapolated to be 4.7T for H//c axis at 23GPa.

To demonstrate the results are highly repetitive, we put results from different measurements on several specimens together. Figure 3 shows the T_c and the carrier density dependence on pressure. The evolution of T_c is shown in figure 3 (a). According to the results from figure 3 (a), we divide the range of the pressure into two regions (ambient phase and high pressure phases). Increasing the pressure from 12.5GPa to 31.9GPa, T_c increases quickly to the highest temperature (around 8.5K), then decreases to near 6.5K when pressure increases to around 21GPa, and then keeps almost a constant. Electrical transport and optical measurement show Bi_2Se_3 is a n-type doped semiconductor.^{24, 26-28} The p-type behavior of Bi_2Se_3 has been induced through slight chemical substitution.^{29, 30} The electron state changes from the hole-dominated to electron-dominated type in Bi_2Te_3 induced by pressure and the T_c dependence on pressure of Bi_2Te_3 is closely related to the change of the differential of hall coefficient over pressure.³¹ In order to study the carrier density change of Bi_2Se_3 we performed the Hall effect measurements from 2GPa to 23GPa with a magnetic field perpendicular to the a-b plane of the sample up to 7T, by sweeping the magnetic field at a fixed temperature (30K) for each given pressure. The Hall coefficient measurements indicate the carrier of crystals used in the experiments is electron-dominated type which do not change over the entire measured pressure range. From several measurements at ambient pressure, we calculated the carrier density to be approximately $10^{18}/\text{cm}^3$. From 2GPa to 23GPa, the carrier density increases by more than two orders of magnitude at temperature 30K as shown in figure 3 (b). Besides, the carrier density increases abruptly around 5.5GPa (ETT pressure) and 12GPa (superconducting onset pressure). It changes

quickly at high pressure phase. Meanwhile, when the carrier density goes up to the maximum value, T_c is the highest too. Therefore, the variation of T_c versus pressure is closely connected with the change of carrier density at pressure.

To investigate the crystal structure evolution as function of pressure, we conducted high pressure x ray diffractions with synchrotron radiation at 9K that is a temperature range near the superconducting transition. At 9 K and pressures below 9.6GPa, Bi_2Se_3 remains ambient phase, but a high pressure phase sets in with further increasing pressure. Phase transitions takes place at around 12GPa and 20GPa, respectively, as shown in figure 4 (a). Figure 4 (b) shows the lattice parameter a , c and volume V versus pressure at ambient pressure phase, which decrease with increasing pressure.

Referring to results of synchrotron radiation with Ref. 22, we infer that Bi_2Se_3 has four phases: ambient phase I from 0 to 12 GPa with rhombohedral $R\bar{3}m$ structure; high pressure phase I (12~20GPa), high pressure phase II (20~30GPa), and high pressure phase III (>30GPa) with monoclinic sevenfold $C2/m$ structure, monoclinic eightfold $C2/c$ structure and BCC $Im\bar{3}m$ structure, respectively.

Figure 5 shows the global phase diagram of n-type Bi_2Se_3 single crystal as function of pressure up to 32GPa. The black and blue balls represent independent experimental data. According to the crystal structure phase transition at 9K at pressures of around 12GPa, 20GPa and >29GPa, respectively, the phase diagram is composed of four areas. Bi_2Se_3 becomes a superconductor at its high pressure phases of HP I, HP II and HP III.

In summary, we found the superconductivity of Bi_2Se_3 at its high pressure phases. The T_c

dependence of pressure is closely dependent of change of carrier density. The x ray diffractions with synchrotron radiation further indicate four crystal structures of Bi_2Se_3 as function of pressure with high pressure states being superconductive.

Acknowledgments

This work was supported by NSF & MOST through research projects. HPSynC is supported as part of EFree, an Energy Frontier Research Center funded by the U.S. Department of Energy under Award DE-SC0001057. HPCAT is supported by DOE-BES, DOE-NNSA (CDAC), and National Science Foundation

References

- ¹B. A. Bernevig, T. L. Hughes, and S. C. Zhang, *Science* **314**, 1757 (2006).
- ²L. Fu and C. Kane, *Phys. Rev. B* **76**, 045302 (2007).
- ³M. Konig, S. Wiedmann, C. Brune, A. Roth, H. Buhmann, L. W. Molenkamp, X. L. Qi, and S. C. Zhang, *Science* **318**, 766 (2007).
- ⁴D. Hsieh, D. Qian, L. Wray, Y. Xia, Y. S. Hor, R. J. Cava, and M. Z. Hasan, *Nature* **452**, 970 (2008).
- ⁵Y. L. Chen, J. G. Analytis, J. H. Chu, Z. K. Liu, S. K. Mo, X. L. Qi, H. J. Zhang, D. H. Lu, X. Dai, Z. Fang, S. C. Zhang, I. R. Fisher, Z. Hussain, and Z. X. Shen, *Science* **325**, 178 (2009).
- ⁶H. J. Zhang, C. X. Liu, X. L. Qi, X. Dai, Z. Fang, and S.C. Zhang, *Nat. Phys.* **5**, 438(2009).
- ⁷Y. Xia, D. Qian, D. Hsieh, L. Wray, A. Pal, H. Lin, A. Bansil, D. Grauer, Y. S. Hor, R. J. Cava, and M. Z. Hasan, *Nat. Phys.* **5**, 398 (2009).

- ⁸X. L. Qi, and S. C. Zhang, *Phys. Today* **63**, 33 (2010).
- ⁹ F. Wilczek, *Nat. Phys.* **5**, 614 (2009).
- ¹⁰ C. Nayak, S. H Simon, A. Stern, M. Freedman, S. Das Sarma Non-Abelian anyons and topological quantum computation. *Rev Mod Phys* **80**, 1083 (2008)
- ¹¹ M. Z. Hasan and C. L. Kane, *Rev. Mod. Phys.* **82**, 3045 (2010).
- ¹² X. L. Qi and S. C. Zhang, *Rev. Mod. Phys.* **83**, 1057 (2011).
- ¹³ P. Larson, V. Greanya, W. Tonjes, R. Liu, S. Mahanti, and C. Olson, *Phys. Rev. B* **65**, 085108 (2002).
- ¹⁴ X. L. Qi, T. Hughes, S. Raghu, and S. C. Zhang, *Phys. Rev. Lett.* **102**, 187001 (2009).
- ¹⁵ L. Fu and C. Kane, *Phys. Rev. Lett.* **100**, 096407 (2008).
- ¹⁶ J. Moore, *Nature Phys.* **5**, 378 (2009).
- ¹⁷ Y. S. Hor, A. J. Williams, J. G. Checkelsky, P. Roushan, J. Seo, Q. Xu, H. W. Zandbergen, A. Yazdani, N. P. Ong, and R. J. Cava, *Phys. Rev. Lett.* **104**, 057001 (2010).
- ¹⁸ J. L. Zhang, S. J. Zhang, H. M. Weng, W. Zhang, L. X. Yang, Q. Q. Liu, S. M. Feng, X. C. Wang, R. C. Yu, L. Z. Cao, L. Wang, W. G. Yang, H. Z. Liu, W. Y. Zhao, S. C. Zhang, X. Dai, Z. Fang, and C. Q. Jin, *Proc. Natl Acad. Sci.* **108**, 24 (2011).
- ¹⁹ S. J. Zhang, J. L. Zhang, X. H. Yu, J. Zhu, P. P. Kong, S. M. Feng, Q. Q. Liu, L. X. Yang, X. C. Wang, L. Z. Cao, W. G. Yang, L. Wang, H. K. Mao, Y. S. Zhao, H. Z. Liu, X. Dai, Z. Fang, S. C. Zhang, and C. Q. Jin, *J. Appl. Phys.* **111**, 112630 (2012).
- ²⁰ S. J. Zhang, X. C. Wang, Q. Q. Liu, Y. X. Lv, X. H. Yu, Z. J. Lin, Y. S. Zhao, L. Wang, Y. Ding, H. K. Mao, and C. Q. Jin, *Europhys. Lett.* **88**, 47008 (2009).

- ²¹H. K. Mao and P. M. Bell, *Rev. Sci. Instrum.* **52**, 615 (1981).
- ²²J. J. Hamlin, J. R. Jeffries, N. P. Butch, P. Syers, D. A. Zocco, S. T. Weir, Y. K. Vohra, J. Paglione, and M. B. Maple, *J. Phys.: Condens. Matter* **24**, 035602 (2012).
- ²³R. Vilaplana, D. Santamaría-Pérez, O. Gomis, F. J. Manjón, J. González, A. Segura, A. Muñoz, P. Rodríguez-Hernández, E. Pérez-González, V. Marín-Borrás, V. Muñoz-Sanjose, C. Drasar, and V. Kucek, *Phys. Rev. B* **84**, 184110 (2011).
- ²⁴N. P. Butch, K. Kirshenbaum, P. Syers, A. B. Sushkov, G. S. Jenkins, H. D. Drew, and J. Paglione, *Phys. Rev. B* **81**, 241301 (2010).
- ²⁵N. R. Werthamer, E. Helfand, and P. C. Hohenberg, *Phys. Rev.* **147**, 295 (1966).
- ²⁶A. B. Sushkov, G. S. Jenkins, D. C. Schmadel, N. P. Butch, J. Paglione, and H. D. Drew, *Phys. Rev. B* **82**, 125110 (2010).
- ²⁷G. S. Jenkins, A. B. Sushkov, D. C. Schmadel, N. P. Butch, P. Syers, J. Paglione, and H. D. Drew, *Phys. Rev. B* **82**, 125120 (2010).
- ²⁸S. Cho, N. P. Butch, J. Paglione, and M. S. Fuhrer, *Nano Lett.* **11**, 1925 (2011).
- ²⁹J. Kašparová, È. Drašar, A. Krejčová, L. Beneš, P. Lošt'ák, W. Chen, Z. H. Zhou, and C. Uher, *J. Appl. Phys.* **97**, 103720 (2005).
- ³⁰Y. S. Hor, A. Richardella, P. Roushan, Y. Xia, J. G. Checkelsky, A. Yazdani, M. Z. Hasan, N. P. Ong, and R. J. Cava, *Phys. Rev. B* **79**, 195208 (2009).
- ³¹C. Zhang, L. L. Sun, Z. Y. Chen, X. J. Zhou, Q. Wu, W. Yi, J. Guo, X. L. Dong, and Z. X. Zhao, *Phys. Rev. B* **83**, 140504 (2011).

Figure captions

FIG.1. (Color) The resistance of Bi_2Se_3 single crystal as function of temperature at ambient pressure phase (a) (with small pressure interval), (b) (with large pressure interval) and high pressure phase showing superconductivity (c). The first superconducting pressure is around 12GPa. (a) and (b) are independent experiments.

FIG.2. (Color) The superconducting transition of Bi_2Se_3 with applied magnetic field H perpendicular to the a - b plane of single crystal at 23GPa (a). The T_c dependence of the magnetic field is showed in (b), and the upper critical fields $H_{c2}(0)$ are extrapolated to be 4.7T at 23GPa.

FIG.3. (Color) The T_c (a) and the carrier density (b) as function of pressure from independent experiments.

FIG.4. (Color) The x-ray diffraction spectra of Bi_2Se_3 at different pressure and $T=9\text{K}$ (a). The wavelength of synchrotron radiation is 0.398\AA . (b) shows the lattice parameter a , c and volume V versus pressure at 9K.

FIG.5. (Color) The phase diagram of n -type Bi_2Se_3 single crystal as function of pressure up to 32GPa. The black and blue balls represent superconducting transition temperature from different experiments.

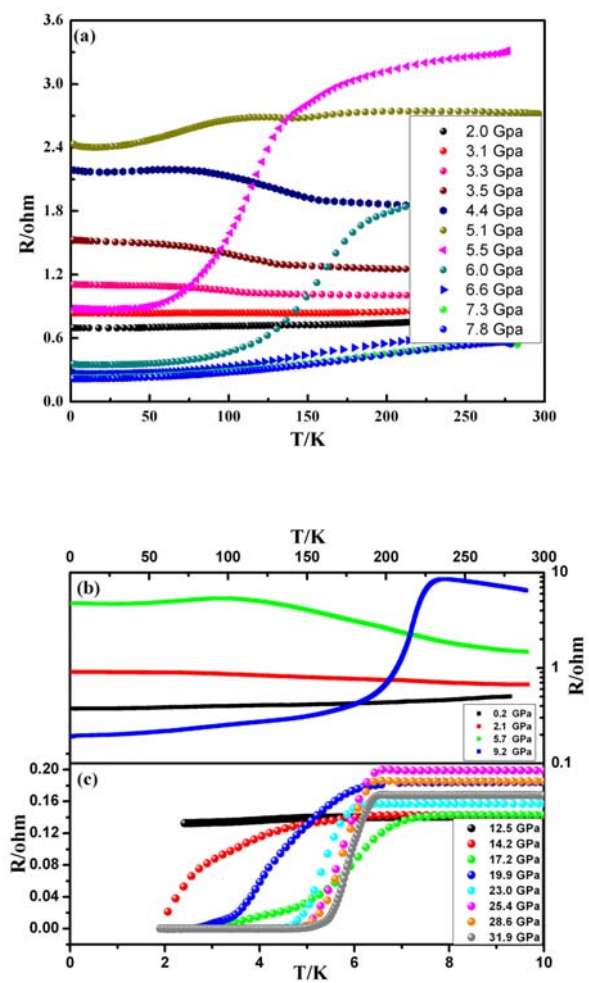


FIG.1.

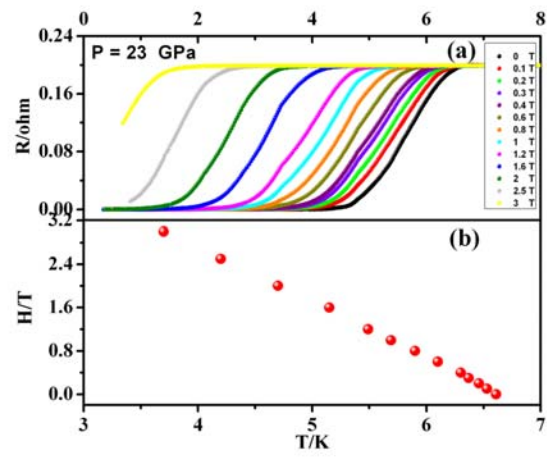


FIG.2

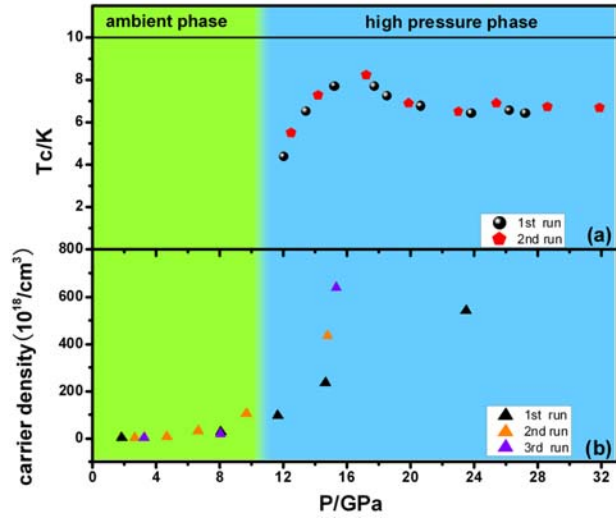


FIG.3

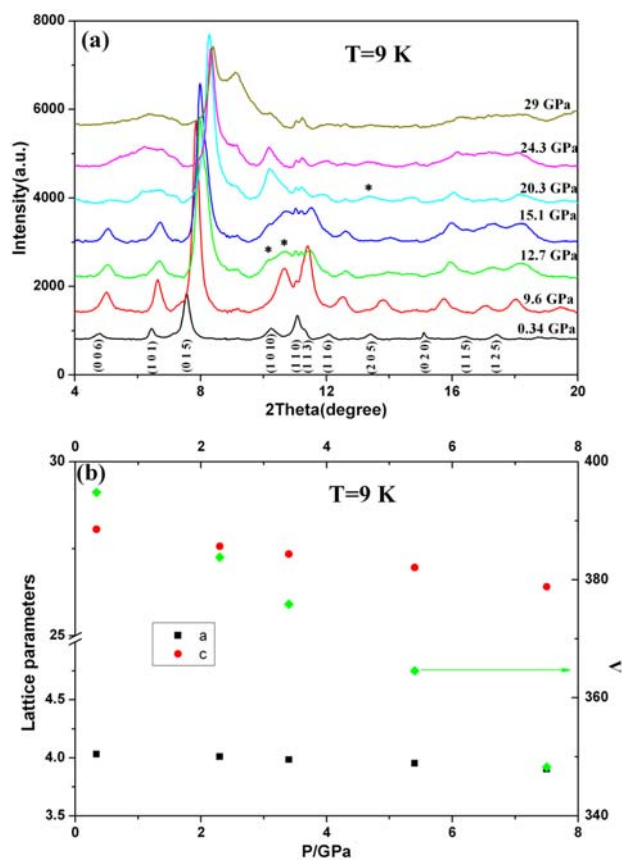


FIG.4

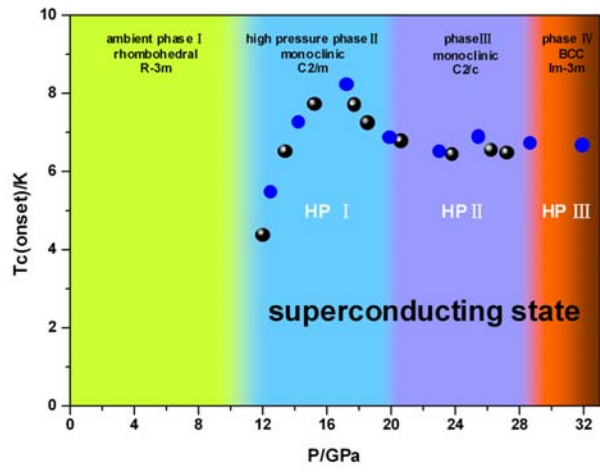


FIG.5.